

First-principles study of the structural properties of Ge

K. J. Chang and Marvin L. Cohen

Department of Physics, University of California, Berkeley, California 94720
and Materials and Molecular Research Division, Lawrence Berkeley Laboratory,
University of California, Berkeley, California 94720

(Received 5 August 1986)

With the use of an *ab initio* pseudopotential method, the structural properties of Ge are investigated at normal and high pressures. The pressure-induced structural phase transitions from cubic diamond to β -Sn, to simple hexagonal (sh), and to double hexagonal close packed (dhcp) are examined. With the possible exception of the dhcp structure, the calculated transition pressures, transition volumes, and axial ratios are in good agreement with experimental results. We find that sh Ge has characteristics similar to those of sh Si; the bonds between hexagonal layers are stronger than intralayer bonds and the transverse phonon modes become soft near the transitions from the sh to β -Sn and the sh to hcp structures. At normal pressures, we compare the crystal energies for the cubic diamond, hexagonal $2H$, and hexagonal $4H$ structures. Because of the similar sp^3 bonds in these structures, the structural energy differences are less than about 14 meV, and the $2H$ and $4H$ phases are metastable with respect to the cubic diamond structure. The equation of state is also presented and compared with experiment.

I. INTRODUCTION

There have been stimulating studies of the high-pressure behavior of Si and Ge. For Si, both experimentally and theoretically, it has been shown that the crystal structure changes from the semiconducting diamond to the metallic β -Sn structure at pressures around 10 GPa.¹⁻⁷ For pressures above 13 GPa, the metallic β -Sn phase transforms into the simple (or primitive) hexagonal (sh) phase and then there is a change into the hexagonal close-packed (hcp) structure above 41 GPa.^{3-5,7,8} The hcp structure for Si was predicted^{6,9} to be a possible high-pressure phase, but the sh phase was not considered in these calculations. The discovery^{3,4} of the sh phase stimulated theoretical studies of its properties. Superconductivity for the sh and hcp phases of Si was predicted^{10,11} and confirmed for both structures by experiments,^{10,12,13} and the superconducting transition temperature of 8.2 K for sh Si (Ref. 10) is among the highest found in nontransition elements.

For Ge, however, for pressures up to 50 GPa, only the diamond to β -Sn transition was observed.^{3,5} Although several close-packed structures, such as face-centered cubic, body-centered cubic, and hcp, were investigated theoretically⁶ as high-pressure candidates; it was shown that the β -Sn structure will not transform into these phases below 100 GPa. Recent pseudopotential calculations¹⁴ performed by the present authors predicted that for higher pressures above 80 GPa, Ge has the same structural sequence, β -Sn to sh to hcp, as that found in Si. These calculations were tested using x-ray diffraction techniques¹⁴ for pressures up to 125 GPa. The predicted properties of the β -Sn to sh transition were found consistent with the x-ray data, but a double hexagonal close-packed (dhcp) structure appears at 102 GPa which is close to the calculated pressure for the sh to hcp transition.

Studies of the structural properties for Si showed that the β -Sn to sh and the sh to hcp phase transitions are most likely associated with soft phonon modes.^{7,15} In this material, the phonon mode softenings result from the weakening of the chemical bonds in particular directions. These soft modes were also found to play an important role in enhancing electron-phonon interactions and superconducting critical temperatures.¹⁰⁻¹² Because of the soft modes near the phase boundaries to the β -Sn and the hcp phases, the sh structure is likely to be unstable. This may account for the observation that the sh structure is rarely found in nature; sh Si and Ge are the only known monatomic systems. Since the coordination number (CN) generally increases with pressure, the structural sequence cubic diamond (CN of 4) to β -Sn (CN of 6) to sh (CN of 8) to hcp or dhcp (CN of 12) is a consistent series. Usually, pressure weakens the chemical bonds, and the resulting metalliclike charge distributions favor close-packed crystal structures.¹⁶

There are many similarities between Si and Ge. Examples include their crystal structures and electronic charge densities. In addition, at similar pressures around 10 GPa, both Si and Ge transform from the diamond to the β -Sn structures. However, for phase transitions between metallic phases, the transition pressures are much higher for Ge than Si.¹⁴ This is inconsistent with the usual empirical finding that transition pressures decrease in going to heavier elements for the same type of phase transitions.¹⁷ With decreasing pressure from the high-pressure phases, Si and Ge were found to form in different metastable structures: a body-centered-cubic structure^{18,19} with 8 atoms per unit cell for Si (BG-8) and a simple-tetragonal structure^{19,20} with 12 atoms per unit cell for Ge (ST-12). Recently, other novel crystalline structures were proposed for these elements by stacking two-dimensionally ordered slabs of atoms in different ways.²¹

Fivefold rings are formed within a slab and this type of ring geometry is found experimentally in $\text{Li}_7\text{Ge}_{12}$ and *allo-Ge* (Ref. 22).

In this paper we report the results of total-energy *ab initio* pseudopotential calculations for studying the structural stability of various phases of Ge at high pressures. Near the phase transitions from the β -Sn to the sh and from the sh to the hcp structures, we investigate the role of soft phonon modes associated with the atomic displacements necessary to induce these transitions. The phase stabilities of the hcp and dhcp structures are discussed based on individual contributions to the total energy. With angular momentum decompositions of the valence wave functions, the role of *d*-state core effects on the metallic phase stability is studied. Furthermore, the cubic diamond, hexagonal *2H* and hexagonal *4H* structures are compared for their phase stabilities at normal pressures. Finally, the equation of state is presented and compared with experiment. In some cases, the results presented here augment those published previously.¹⁴

II. METHOD

The calculations are based on the *ab initio* pseudopotential-total-energy method.²³ The exchange-correlation functional is approximated by the Wigner interpolation formula.²⁴ Nonlocal pseudopotentials having *s*, *p*, and *d* symmetry are generated,²⁵ these pseudopotentials were successfully used in previous calculations for the structural and dynamical properties of Ge.^{6,26} For insulators and semiconductors, the band gaps are usually smaller by about 30–50% when the local-density approximation is used.²⁷ It has been shown that relativistic and spin-orbit coupling effects are large on some conduction bands of heavy elements; the band gap for Ge is found to be almost zero.²⁸ However, we find that including the relativistic effects does not affect the structural properties for Ge significantly. For atomic and solid-state calculations, spin-orbit coupling effects are not included. Previous calculations²⁹ have shown that the ground-state properties even for compounds with heavier atoms do not change significantly by neglecting the spin-orbit coupling.

We calculate the crystal energies self-consistently in momentum space.³⁰ The (pseudo) valence wave functions are expanded in a plane-wave basis set with a kinetic energy cutoff of up to 11.5 Ry. The summation over the Brillouin zone is carried out using a uniform grid of *k* points for each phase, and the cubic diamond (CD), hexagonal diamond (*2H*), hexagonal *4H*, β -Sn, simple hexagonal, hexagonal close-packed, double hexagonal close-packed, body-centered-cubic (bcc), and face-centered-cubic (fcc) structures are considered. To compare the total energies for the CD, *2H*, and *4H* structures, we used an equivalent set of *k* points on the hexagonal plane of the Brillouin zone by choosing hexagonal cells along the cubic [111] axis. We find that the total energy is less sensitive to the set of *k* points along the *c* axis. A similar method was used in a previous study of stacking faults in Si.³¹ The same procedure in sampling the *k* points is used here for the hexagonal metallic phases, sh, hcp, and dhcp. For the metallic phases, larger numbers of *k* points are necessary

to ensure good energy convergence. Grids of 75, 75, 150, 146, and 140 sampling points in the irreducible Brillouin zone are chosen for the β -Sn, hcp, sh, fcc, and bcc structures, respectively. The resulting maximum error in the total energy is within 0.5 mRy per atom.

The calculated energies are fitted to Murnaghan's equation of state.³² Thus, the ground-state properties, such as equilibrium lattice constants (*a*), bulk moduli (B_0), and pressure derivatives of the bulk moduli (B'_0), are obtained. The structural phase stability under pressure is examined by comparing the Gibbs free energies computed from the sum of the total energy and the mechanical work (pressure times volume) at zero temperature. Since pressure or variations of volume change the electron charge distributions, relaxations of the bond lengths are necessary for noncubic structures. For the tetragonal and hexagonal phases, we optimize the *c/a* ratios using energy minimization.

The phonon frequencies are calculated within the frozen-phonon approximation.²⁶ This approximation freezes in atomic motions corresponding to a phonon distortion. The difference in the calculated energies for the equilibrium and the distorted lattices gives the corresponding phonon frequency. Here, we choose the phonon modes which are associated with the phase transitions. For the β -Sn to sh transition, the transverse acoustic mode for $\mathbf{q}||[011]$ is used in the sh structure, while for the sh to hcp transition, the TA mode for $\mathbf{q}||[001]$ is chosen.

To represent the pressure effects, we reduce the volume up to 47% of the equilibrium volume. The present potentials only treat *sp* valence electrons assuming that *3d*-state core radii of the ions are well separated. However, further compression of the volume below the minimum considered here should take into account core-core overlap effects because of the large core radius of the Ge atom.

III. RESULTS

A. Structural stability at high pressures

With increasing pressure, the structural transitions for Si occurs as follows: from cubic diamond to β -Sn to sh to hcp.^{1–9} The coordination number increases in this series. Similar transitions for Ge were predicted by theoretical calculations and confirmed by experiment.¹⁴ Since the CD structure is semiconducting, the first transition into the β -Sn phase corresponds to the pressure-induced metallization of Ge. Usually, the bond charges move into the interstitial regions under pressure. When the volume is reduced by about 20% at the phase transition,^{1–7} the contraction of one of the cubic diamond axes increases the probability that atoms will form two extra bonds in the interstitial regions. The resulting sixfold β -Sn structure causes band overlap and thus a metallic state is likely. With further increase of pressure, the metallic β -Sn phase successively changes into the close-packed structures having higher coordination numbers. The Ewald energy decreases for these highly coordinated structures⁶ and the structures are stabilized.

In Figs. 1 and 2, the calculated total energies are fitted to the Murnaghan equation of state for various crystal

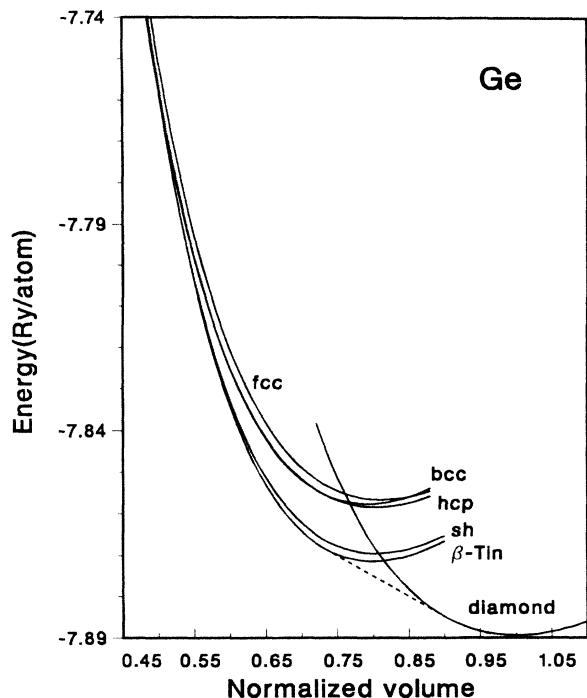


FIG. 1. Crystal energies versus volume normalized by the calculated equilibrium volume of 22.5616 \AA^3 for the cubic diamond phase in Ge.

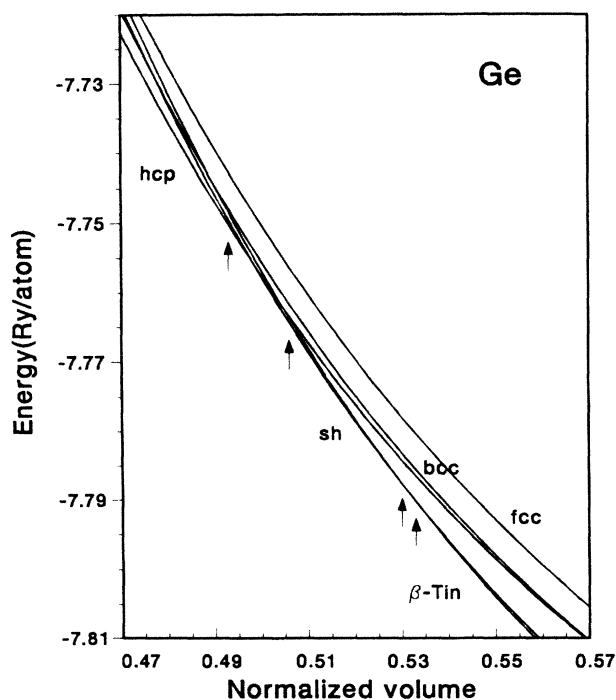


FIG. 2. Detailed structure of the curves in Fig. 1 near the phase transitions. The arrows indicate the transition volumes for the β -Sn to sh and the sh to hcp transitions; numbers positioning the arrows are given in Table II.

structures and are compared as a function of volume. Our calculated values for a , B_0 , and B'_0 for the CD and β -Sn phases are listed in Table I and compared with experiments and other calculations. We find that the results of the calculations for the ground-state properties are consistent with previously calculated results^{6,33} and are also in good agreement with the measured values. Including relativistic effects, the ground-state properties are found to change slightly; less than 0.5% for a and 4% for B_0 . With decreasing volume, the calculated structural transformations from CD to β -Sn, to sh, and to hcp occur. The ordering of the structural transitions between β -Sn, sh, and hcp is the same as that found in Si, while the transition pressures between these structures are higher for Ge. The calculated transition pressures and volumes are listed in Table II for the CD to β -Sn, β -Sn to sh, and sh to hcp transitions, and these values are compared with experiments and other calculations.

For the semiconducting metallic transition from CD to β -Sn, the transition occurs at 9.5 GPa along the common tangent (dashed line) of the lowest two energy curves. The computed transition pressure is in good agreement with the measured values around 10 GPa and is consistent with previously calculated values.^{6,33} The calculated discontinuous change of 16% in volume also agrees well with the measured values. We find that the relativistic effects lower the diamond to β -Sn transition pressure by 0.8 GPa, while its transition volumes are almost the same. The transition pressure for Ge is very close to that of Si, as expected from band-structure arguments since the pressure-induced metallization plays a dominant role in the phase transition for both elements. The pressure coefficients³⁴ of the conduction-band energies are almost the same for both semiconductors. The effect of pressure is normally represented by the decrease of the lowest conduction-state energy at the X point and for both Si and Ge the coefficient was found to be about -15 meV/GPa .³⁵ The energy difference of 1.3 eV between the

TABLE I. Calculated lattice constants, bulk moduli, and their pressure derivatives for the cubic diamond and β -Sn phases.

| | a_0 (\AA) | B_0 (GPa) | B'_0 |
|---------------|------------------------|-------------------------|------------------|
| | Cubic diamond | | |
| Present calc. | 5.651 | 74 | 3.7 |
| | 5.637 ^a | 71 ^a | 3.7 ^a |
| Other calc. | 5.655 ^b | 73 ^b | 3.9 ^c |
| | 5.62 ^c | 78 ^c | 4.5 ^d |
| Expt. | 5.652 ^d | 77 ^d | |
| | β -Sn | | |
| Present calc. | 5.082 | 90 | 3.7 |
| Expt. | | 91 ± 1 ^e | 4.0 ^e |

^aRelativistic effects are included.

^bReference 6.

^cReference 33.

^dSee references in Ref. 6.

^eReference 5.

TABLE II. Transition pressures and transition volumes for the cubic diamond to β -Sn, β -Sn to sh, and sh to hcp (dhcp in experiment) transitions. The volumes are normalized by the calculated equilibrium volume of 22.5616 \AA^3 per atom for the cubic diamond structure. The results are compared with experiments and other calculations.

| | V_t (CD) | V_t (β -Sn) | V_t (sh) | V_t (hcp) | P_t (GPa) |
|---|--------------------|----------------------|--------------------|--------------------|-------------------|
| Cubic diamond \rightarrow β -Sn | | | | | |
| Present calc. | 0.900 | 0.731 | | | 9.5 ± 0.3 |
| | 0.897 ^a | 0.732 ^a | | | 8.7 ± 0.3^a |
| Other calc. | 0.895 ^b | 0.728 ^b | | | 9.6 ^b |
| | 0.887 ^c | 0.712 ^c | | | 9.8 ^c |
| Expt. | 0.895 ^d | 0.74 ^d | | | 10.3 ^d |
| | 0.903 ^e | 0.732 ^e | | | 10.6 ± 0.1^e |
| | 0.910 ^e | 0.760 ^e | | | 9.8 ± 0.2^e |
| β -Sn \rightarrow sh | | | | | |
| Present calc. | | 0.533 | 0.530 | | 84 ± 10 |
| Expt. | | 0.567 ^f | 0.562 ^f | | 75 ± 3^g |
| sh \rightarrow hcp | | | | | |
| Present calc. | | | 0.506 | 0.493 | 105 ± 2 |
| Expt. ^h | | | 0.523 ^f | 0.467 ^f | 102 ± 5^g |

^aRelativistic effects are included.

^bReference 6.

^cReference 33.

^dReference 3.

^eReference 5.

^fReference 37.

^gReference 14.

^hExperimentally, the dhcp structure was found to be more stable.

top valence band at the Γ point and the bottom conduction band at the X point is almost the same for Si and Ge.³⁶ Therefore, the band closing under pressures proceeds in a similar way and the transition pressures are also found to be similar. The CD to β -Sn transition, however, occurs with a discontinuous change of volume before the conduction band meets the valence band.

The β -Sn to sh transition is a metallic-metallic phase transition and its transition pressure is higher for Ge than for Si. The sh phase is found to be stable at 84 ± 10 GPa and the crystal volume changes by 0.3% of V_0 (from 0.533 to 0.530 V_0), where V_0 is the equilibrium volume in the diamond structure. Because the energy curves for the β -Sn and sh structures are very close and sharply rising for a wide range of volume, the calculated pressure is found to vary by 10 GPa when the sh energy changes by 0.5 mRy per atom. Considering this sensitivity to the details of the curves, the agreement of the transition pressure and volume with experiment is good; the measured transition pressure is 75 ± 3 GPa and the change of volume is less than 0.5% of V_0 (Ref. 14).

For higher pressures in the megabar range, the theoretical calculation predicted a transformation into the hcp structure at 105 ± 2 GPa, while the experiment found the dhcp phase to be more stable at 102 ± 5 GPa (Ref. 14). At the sh to hcp transition, the volume is found to change by 1.3% from 0.506 to 0.493 V_0 . Experimentally, the sh to dhcp transition was observed with a discontinuous change of volume of 5.6%; this value for volume is larger

than the calculated value. We find that the dhcp structure is metastable with respect to the hcp structure with small energy differences of about 50 to 70 meV per atom. For Si, we find the difference of the energies to be 15 to 30 meV. Details of the phase stability of these hexagonal structures will be discussed later.

In Table III, the calculated c/a ratios are compared with the measured values for the tetragonal and hexagonal structures. For the tetragonal β -Sn phase, the axial ratio is almost constant for a wide range of its structural stability and the calculated value of 0.55 ± 0.005 is in good agreement with the measured values of around 0.55. For the sh phase, the calculated c/a ratio is 0.945 ± 0.004 and this is close to the measured value of 0.930 ± 0.007 . The computed axial ratios for the hcp and dhcp structures are similar: 1.645 and 1.640 for the c/a of the hcp and for the $c/2a$ of the dhcp phases, respectively. However, these values are a little smaller than the measured values of 1.688 ± 0.008 for the $c/2a$ of the dhcp phase. Experimentally, the axial ratio for the dhcp structure was found to decrease slightly with increasing pressure,³⁸ similar behavior was also found in our calculations for both the hcp and dhcp phases. The calculated axial ratios for non-cubic structures of Ge are similar to Si. This is expected because the axial ratios are primarily determined by the Madelung energy. We find that for Ge the use of only the Ewald energy gives reasonable estimates of the axial ratios: 0.545, 0.929, 1.636, and 1.634 for the β -Sn, sh, hcp, and dhcp structures, respectively.

TABLE III. Axial ratios for the β -Sn, sh, hcp, and dhcp structures of Ge.

| | β -Sn (c/a) | sh (c/a) | hcp (c/a) | dhcp ($c/2a$) |
|---------------|-----------------------|---------------------|-------------------|---------------------|
| Present calc. | 0.55 ± 0.005 | 0.945 ± 0.004 | 1.645 ± 0.005 | 1.640 ± 0.005 |
| Other calc. | 0.55 ± 0.02^a | | | |
| Expt. | 0.551^b | | | |
| | 0.548 ± 0.002^c | | | |
| | 0.554 ± 0.006^c | | | |
| | 0.550 ± 0.008^d | 0.930 ± 0.007^d | | 1.688 ± 0.008^e |

^aReference 6.^bReference 38.^cReference 5.^dReference 14.^eReference 37.

It is generally observed experimentally that the equivalent phase-transition pressure becomes lower when going to a heavier element in a given series of the Periodic Table.¹⁷ This rule includes the metallic to metallic and semiconducting to metallic transitions. Since the β -Sn to sh and sh to hcp transitions for Ge occur at higher transition pressures compared to Si; this represents a departure from the empirical rule. The origin of the high transition pressures between metallic phases of Ge appears to be connected with the large $3d$ -state core radius for the Ge atom. Compared to Si, the minimum energy volumes for Ge (see Fig. 1) are almost the same for the metallic β -Sn, sh, and hcp phases; for Si this volume decreases when going to the highly coordinated structures from β -Sn to sh to hcp.^{6,7} This difference in behavior is probably related to the $3d$ bands in Ge. The d -state pseudopotential in Ge is more repulsive than that of Si because of the occupied $3d$ state in the core.⁶ For both Si and Ge, the energies for the β -Sn and sh phases are close and thus the small change in energy in either phase produces a large change of the transition pressure. However, a constant shift of the sh curve in Si to higher energy, which was attempted⁸ to explain a possible high transition pressure for Ge, does not represent this core effect. A more appropriate approach is to note that the sh and hcp curves of Ge resemble the curves of Si shifted to higher volumes. This shift results from the d -core repulsion and produces a higher

transition pressure.

The highly coordinated structures have smaller charge-density concentrations and longer nearest-neighbor distances for fixed volumes. Therefore, the sh phase has a larger concentration of d -symmetry valence states than the β -Sn structure, as shown in Tables IV and V. This was also found in a previous calculation for Si.⁸ Compared to Si at similar pressures, the sh phase of Ge is found to have a much lower concentration of d -symmetry states: 0.39 and 0.49 electrons per Ge and Si atoms, respectively, near 12 GPa. Although the Ewald energy favors the highly coordinated sh phase, a large electronic energy caused by the reduction of the d -symmetry valence states destabilizes the sh phase for Ge over a wide range of pressure. With increasing pressure, the d -valence state contribution is found to increase and near the β -Sn to sh phase transition it becomes close to that of Si (0.49 electrons per atom) at the same phase transition (see Tables IV and V).

B. Phases at pressures above 1.3 Mbar

For Si, the theoretical calculations^{7,9} predicted that the hcp structure transforms into the fcc phase around 1 Mbar. However, x-ray diffraction measurements have been made only up to 50 GPa.³⁻⁵ If we assume that Ge behaves in a similar manner to Si above 1 Mbar, the hcp

TABLE IV. Angular momentum decompositions of the valence electron wave functions for the β -Sn and sh phases of Si. Numbers of electrons for individual states are denoted by N_s , N_p , and N_d , where s , p , and d denote the angular momentum states. Charges are normalized to four electrons per atom.

| P (GPa) | N_s | N_p | N_d |
|-----------|-------|-------------|-------|
| | | β -Sn | |
| 12.0 | 1.37 | 2.16 | 0.47 |
| 18.4 | 1.35 | 2.16 | 0.49 |
| 30.5 | 1.33 | 2.17 | 0.50 |
| | | sh | |
| 12.0 | 1.37 | 2.14 | 0.49 |
| 18.4 | 1.34 | 2.15 | 0.51 |
| 30.5 | 1.32 | 2.15 | 0.53 |

TABLE V. Angular momentum decompositions of the valence electron wave functions for the β -Sn and sh phases of Ge. Numbers of electrons for individual states are denoted by N_s , N_p , and N_d , where s , p , and d denote the angular momentum states. Charges are normalized to four electrons per atom.

| P (GPa) | N_s | N_p | N_d |
|-----------|-------|-------------|-------|
| | | β -Sn | |
| 12.0 | 1.49 | 2.13 | 0.38 |
| 50.0 | 1.41 | 2.17 | 0.42 |
| 84.0 | 1.37 | 2.19 | 0.44 |
| | | sh | |
| 12.0 | 1.51 | 2.10 | 0.39 |
| 50.0 | 1.42 | 2.14 | 0.44 |
| 84.0 | 1.37 | 2.16 | 0.47 |

structure will appear and then transform into the fcc structure. However, this transition pressure is expected to be higher than that found in Si since the energy curves change rapidly for a small range of volume as seen in the β -Sn to sh and sh to hcp transitions. Our calculations show that for Ge both the fcc and bcc phases are higher in energy than the hcp structure up to the volume of $0.47V_0$ considered here (see Fig. 2). Since the transition volume was predicted to be about $0.46V_0$ for the hcp to fcc transition in Si,^{7,9} we expect that the transition volume for Ge will be lower and the transition pressure will be above 1.5 Mbar because the transition volume between metallic phases for Ge is smaller. To compute the properties of the hcp to fcc or bcc phase transition, further studies which include core-core overlap interactions when compressing the volume below $0.47V_0$ are necessary.

C. Equation of state

Figure 3 shows the calculated equation of state for Ge for various phases. By differentiating the total-energy curves in Fig. 1, the volume versus pressure curve is derived and compared with recently measured equations of state. In the region of low pressures below 100 GPa, the agreement is good. However, above 100 GPa there is a constant deviation between the theoretical and experimental³⁷ equations of state. We may consider two possible sources for the discrepancy: nonhydrostatic pressure distributions for high pressures in the experiments and/or theoretical calculational errors that may arise from neglecting core-core overlap. As discussed earlier, the dhcp structure was observed as a stable phase above 102 GPa while the theory predicted the hcp phase to be more stable. Since the measured value of the change of volume is larger at the sh to dhcp transition, the measured volumes for the dhcp structure is lower. Therefore, above 100 GPa there is a constant difference between the two curves for the equation of state.

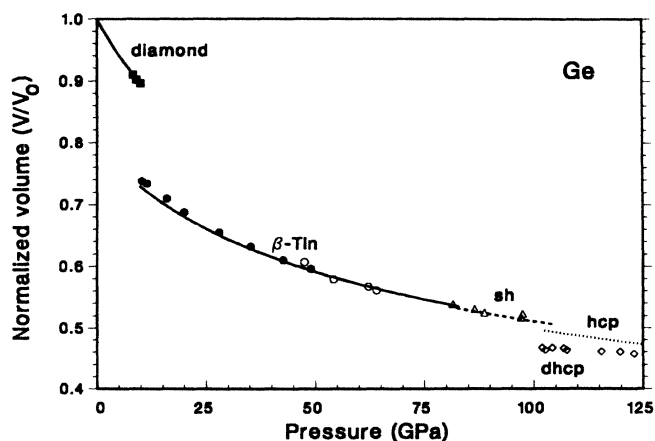


FIG. 3. Equations of state for Ge for pressures up to 125 GPa. Lines denote the calculated curves. Experimental data are represented by points; shaded points are from Ref. 3 and open points are from Ref. 37.

D. Phase stability of hexagonal and double hexagonal close-packed structures

The hcp and dhcp structures differ only in the stacking of the hexagonal close-packed layers: $ABAB\dots$ for the hcp structure and $ABAC\dots$ for the dhcp structure. As illustrated in Fig. 4, the B atoms in the hcp phase have the same configuration of A atoms as the B atoms in the dhcp structure. In contrast, the atoms in the second-nearest layers produce different force fields for B atoms in the two structures because of the different bond lengths. Since the distance between the B atoms in the hcp phase is shorter than that between the C and B atoms of the dhcp phase, the Madelung (Ewald) energy favors the dhcp structure. However, the total energy for hcp Ge was found to be lower by 50 to 70 meV per atom than the dhcp structure. This results from the lower electron-ion interaction energy for the B atoms in the hcp phase compared to the same B atoms in the dhcp phase. Since the bond lengths to the second-nearest atoms are shorter in the hcp phase, the potential fields around the atom are more attractive and the resulting lower electron-ion interaction energy overshadows the Madelung energy, stabilizing the hcp structure. We find that this hcp phase stability appears for both Si and Ge and does not change with the inclusion of relativistic effects in the ionic potentials.

A new intermediate phase was reported in Si between 36 and 40 GPa where the sh to hcp phase transition occurs.³ The new phase was labeled as the Si-VI phase and it disappears for pressures above 41 GPa. Recent reanalysis¹⁴ of the x-ray diffraction pattern of the new phase suggests that the Si-VI phase can be identified as

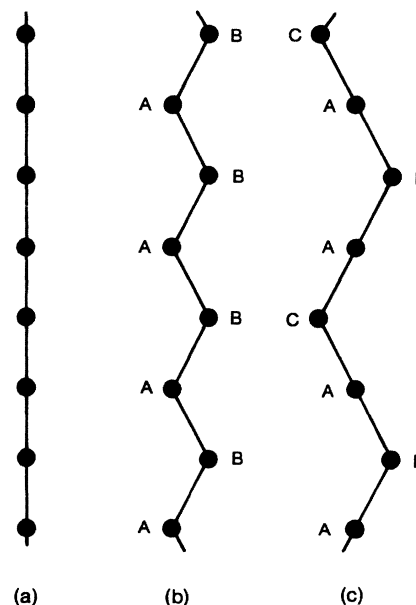


FIG. 4. Stacking sequences of the hexagonal close-packed layers for the (a) sh, (b) hcp, and (c) dhcp structures along the [001] direction. Atoms in different stacking patterns are distinguished by A , B , and C .

dhcp with $c/2a = 1.698$. For Ge, the same x-ray diffraction pattern indexed by the dhcp structure was observed¹⁴ for pressures above 1.02 Mbar and up to 1.25 Mbar. This value is the maximum pressure achieved in the experiment. The dhcp structure produces extra peaks in the diffraction pattern in addition to all the peaks of the hcp structure. However, the modified relative intensities of the peaks suggest the presence of numerous stacking faults.¹⁴ The measured axial ratio $c/2a$ for dhcp Ge is 1.688 ± 0.008 up to 125 GPa and this value is close to that of the Si-VI phase. If the dhcp phase is stable for both Si and Ge, the ordering of the structural sequence of transformations from dhcp to hcp is opposite to the case of trivalent rare earths³⁹ which have the order hcp \rightarrow Sm-type \rightarrow dhcp \rightarrow fcc.

The hcp and dhcp structures can be formed displacively via different phonon modes from the sh phase, accompanied by a reduction in the c/a ratio, as shown in Fig. 4. The transverse acoustic mode for $\mathbf{q} \parallel [001]$ is associated with the sh to hcp transition, while the sh to dhcp transition is related to the TA mode for $\mathbf{q} \parallel [00\frac{1}{2}]$. We find that for Ge the phonon frequency for the TA mode at $\mathbf{q} \parallel [001]$ becomes soft near the sh to hcp phase transition as in the case of Si. In contrast, the frequency of the TA mode at $\mathbf{q} \parallel [00\frac{1}{2}]$ does not decrease with increasing pressure, as shown in Table VI. This suggests that the sh phase is more likely to transform to the hcp structure than the dhcp structure. This effect also appears in the total-energy calculations since the hcp structure is lower in energy than the dhcp phase. However, we find for Si that despite the stable phonon frequency for $\mathbf{q} \parallel [00\frac{1}{2}]$ the phonon linewidth rapidly increases for pressures above 36 GPa near the sh to hcp phase transition.⁴⁰ This increase of the phonon linewidth is almost twice as large as that calculated for $\mathbf{q} \parallel [001]$. Since the calculated phonon linewidth only includes electron-phonon scattering, the measurements of the lifetime for the transverse phonon

would give detailed information about the phonon-phonon anharmonic contributions.

Another possible effect on the phase stability of dhcp with respect to the hcp structure is the long-range force which can be produced by the stacking faults at the transition. Since different stackings of hexagonal layers do not require much structural energy, stacking faults along the axial direction can exist. In fact, the presence of stacking faults are suggested by x-ray diffraction patterns.^{3,14} If phase domains are created when the sh to hcp transition occurs, the stackings of the layers on the domain boundaries can locally resemble that of the dhcp phase. For Ge, we can also consider d -state core effects. Since the size of the Ge core is relatively larger than Si, compressions of the volume below $0.47V_0$ give rise to core-core overlap. Furthermore, the core polarization for the Ge atom is not negligible and the normally negligible van der Waals interactions between cores might be effective for such compressed volumes.⁴¹ These core effects are negligible for Si since the cores are well separated even if the volume is compressed up to $0.4V_0$ and the core polarization is small because of the small core radius. Therefore, if the reason for the dhcp phase stability is the same for Si and Ge, core effects may not be significant in stabilizing the dhcp structure.

E. Cubic diamond α , hexagonal $2H$, and hexagonal $4H$ structures at normal pressures

It is interesting to compare the α , $2H$, and $4H$ crystal structures and the corresponding total energies for Ge. In recent experiments,²² novel metastable modifications of Ge were found. Using chemical processes rather than pressure, single crystals of *allo*-Ge are formed from $\text{Li}_7\text{Ge}_{12}$; its crystal structure was found to be orthorhombic containing 128 atoms in a cell. On heating, *allo*-Ge transforms first into the $4H$ phase at 420 K and then into the α phase at 770 K. The hexagonal $2H$ and $4H$ structures are well known polytypes of SiC.

The stacking pattern for the cubic diamond structure along the $[111]$ direction (see Fig. 5) is obtained when the hexagonal layers are sequenced as $AaBbCc\dots$, where the atomic layer a (b or c) is placed on the top of layer A (B or C) with a separation of true standard bond length. This structure has six atoms per hexagonal unit cell. The stacking sequences for the $2H$ and $4H$ structures have the patterns of $AaBb\dots$ and $AaBbAaCc\dots$, respectively, as shown in Fig. 5. Comparing the stacking patterns, the $2H$ and $4H$ structures are similar to the hcp and dhcp structures, respectively, while there are twice as many atoms in the $2H$ and $4H$ structures because of the extra atomic layers on top of each layer. Since these extra atoms form tetrahedral bonds, the covalent sp^3 bonds (CN of 4) for the $2H$ and $4H$ phases favor the semiconducting state, while the hcp and dhcp structures with the higher coordination number (CN of 12) are metallic.

The total energies for the α , $2H$, and $4H$ phases are computed and compared using the hexagonal unit cells. Since the hexagonal planes in the Brillouin zone are equivalent, the same set of \mathbf{k} -point sampling on this plane is used to reduce the calculational errors arising from the

TABLE VI. Calculated transverse acoustic phonon frequencies for \mathbf{q} 's $\parallel [011]$, $[001]$, and $[00\frac{1}{2}]$ for sh Ge. Frequencies are in units of 10^{13} rad/sec.

| \mathbf{q} | P (GPa) | Frequency |
|---------------------|-----------|-------------------|
| [011] | 58 | 0.76 ^a |
| | 67 | 1.18 |
| | 78 | 1.47 |
| | 91 | 1.51 |
| | 96 | 1.52 |
| [001] | 90 | 1.18 |
| | 96 | 1.13 |
| | 102 | 1.07 |
| | 105 | 0.78 |
| | 120 | 0.61 |
| [00 $\frac{1}{2}$] | 90 | 1.01 |
| | 102 | 1.01 |
| | 105 | 1.01 |

^aThe calculated frequency is imaginary.

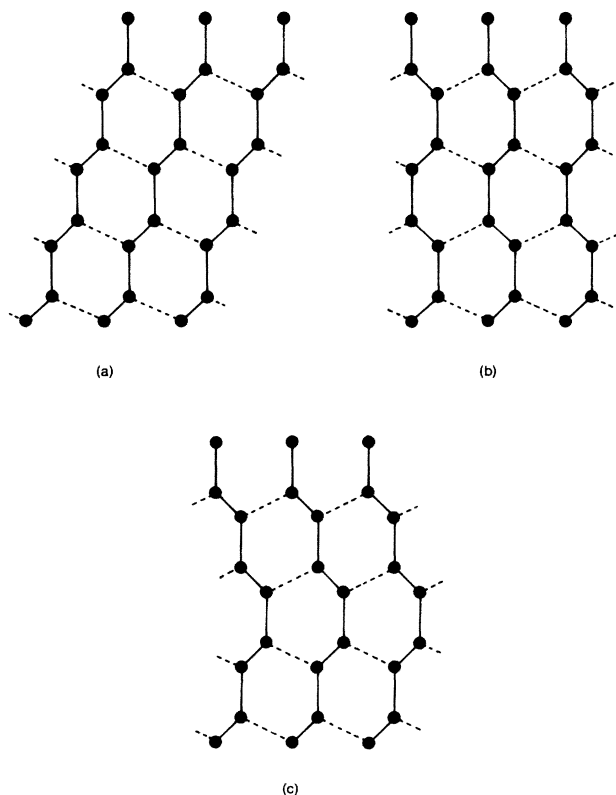


FIG. 5. Stacking sequences for the (a) cubic diamond, (b) hexagonal $2H$, and (c) hexagonal $4H$ structures along the $[111]$ direction of the cubic lattice. Circles and lines represent the atoms and the bonds, respectively.

finite grids. Because the size of the unit cell along the c axis is different for each phase, the \mathbf{k} -point sampling along the c axis is not equivalent. However, we find that the total energy is not sensitive to the grids along this direction, and is stable within to 0.3 mRy per atom for different sets of grids along the z direction (c axis) with the same grids on the xy plane.

Using equivalent sets of \mathbf{k} -point sampling in the irreducible Brillouin zones, the α phase is found to be the most stable phase; the total energy for this structure is lower by 5 and 14 meV per atom than those for the $4H$ and $2H$ phases, respectively. The energy difference between the α and $2H$ phases is in good agreement with the previously calculated result⁶ and this value is close to that found in Si.^{6,7} Because of the small energy difference, the $2H$ and $4H$ structures are suggested to be metastable. The hexagonal structure has been found even in experiments not employing chemical processes.⁴² It was shown that when a thin film of amorphous Ge is crystallized by electron-beam heating, the polycrystalline matrix has a mixture of hexagonal and diamond structures.²¹ Recent calculations²¹ suggested that for both Si and Ge an orthorhombic unit cell with 20 atoms (O-20) is the most energetically favored structure among novel complex crystalline forms built in slab geometries; the energy of the O-20 structure is higher by about 30 meV compared to the α phase.

F. Soft phonon modes

Structural phase transitions are often induced by soft phonon modes. In the case of second-order phase transitions,⁴³ the phonon frequency becomes zero at the transition; for example, this is the case for the optic phonon frequency at the zone center for ferroelectrics. Because the lattice is unstable, the crystal structure changes displacively. In previous studies^{7,15} for Si, it was shown that the β -Sn and hcp structures can be obtained displacively from the sh phase, with appropriate modifications of the axial ratios. There exist the soft phonon modes associated with the atomic motions necessary to bring the sh structure into the β -Sn and hcp structures; the sh to β -Sn transition is related to the TA mode for $\mathbf{q} \parallel [011]$, while the TA mode for $\mathbf{q} \parallel [001]$ induces the sh to hcp transition. Although these phonon frequencies decrease when the pressure is close to the transition pressure, their values are

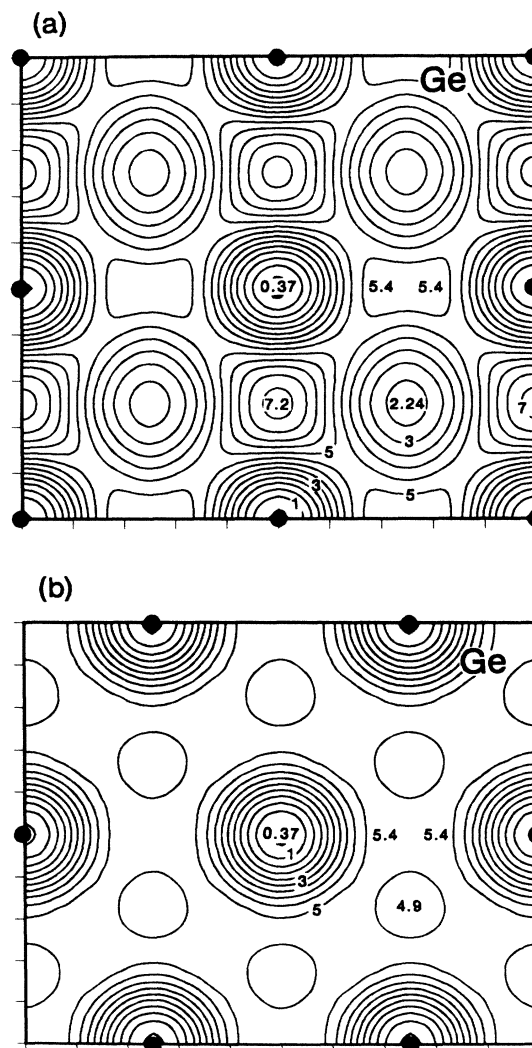


FIG. 6. Contour plots of the valence charge densities in the (a) $[10\bar{1}0]$ and (b) $[0001]$ planes for the sh phase. An atomic volume of 11.4843 \AA^3 is used. Steps are in units of one-half electron per cell volume.

found to be finite. This is because additional lattice distortions change the axial ratios and effectively reduce the energy barriers; these energy barriers were found to be small for both the β -Sn to sh and the sh to hcp transitions,^{7,8} suggesting that the transitions are displacive for both cases.

Similarly, the same phonon modes for Ge cause the structural transitions similar to those found in Si. The calculated values for the frequencies of these modes are listed in Table VI and compared for several different pressures. We find that near the phase transitions the corresponding phonon frequencies decrease but do not become zero, just as in the case of Si. By varying the c/a ratios for each phonon displacement, we calculated energy barriers of less than 10 meV for the β -Sn to sh transition and less than 20 meV for the sh to hcp transition.

G. Valence electron charge distributions

In Fig. 6, the calculated valence charge densities are shown for the sh structure of Ge. Compared to the charge density in the hexagonal plane, the axial direction has a larger pileup of charge and thus the chemical bonds between layers are stronger. This behavior was also found for the sh structure of Si.⁷ The strong bonds connecting layers are covalent and hence differ from the weak π bonds in graphite.⁴⁴ The axial ratio for the sh phase is slightly smaller than 1 because of the stronger bonds between layers. Thus, atomic distortions within layers require less energy and produce phonon softening for this mode.

IV. CONCLUSION

We have studied the phase stabilities and the solid-solid phase transitions for Ge at normal and high pressures. The pseudopotential-total-energy calculations for Ge yield

a pressure-induced structural sequence cubic diamond to β -Sn, to sh, to hcp, which is the same as that found for Si. Relativistic effects are found to change the ground-state properties only slightly, despite the almost zero band gap for the diamond cubic phase of Ge caused by the use of the local-density approximation. Although experimentally the dhcp structure was found to be more stable with respect to the hcp structure above 102 GPa, the difference of two crystal energies is estimated to be small, suggesting that the dhcp structure may be metastable. We also suggest that stacking faults may be the origin of the dhcp phase stability.

At normal pressures, the hexagonal $2H$ and $4H$ structures are calculated to be metastable with respect to the cubic diamond phase. The energies for creating stacking faults are estimated to be less than 14 meV from the semiconducting diamond to the hexagonal $2H$ and $4H$ phases and less than 70 meV from the metallic hcp to the dhcp phases. We have shown that the sh structure for Ge has characteristics similar to the case of sh Si; bonds between layers are stronger with respect to those within layers and the transverse modes become soft near the phase boundaries.

ACKNOWLEDGMENTS

We would like to thank Professor A. L. Ruoff and Dr. Y. K. Vohra for providing information about their experimental data. This work was supported by National Science Foundation Grant No. DMR-83-19024 and by the Director, Office of Energy Research, Office of Basic Energy Sciences, Materials Sciences Division of the U.S. Department of Energy under Contract No. DE-AC03-76SF00098. Cray computer time was provided by the Office of the Energy Research of the U.S. Department of Energy.

-
- ¹S. Monomura and H. G. Drickamer, *J. Phys. Chem. Solids* **23**, 451 (1962).
- ²G. J. Piermarini and S. Block, *Rev. Sci. Instrum.* **46**, 973 (1975); W. A. Weinstein and G. J. Piermarini, *Phys. Rev. B* **12**, 1172 (1975).
- ³H. Olijnyk, S. K. Sikka, and W. B. Holzapfel, *Phys. Lett.* **103A**, 137 (1984).
- ⁴J. Z. Hu and I. L. Spain, *Solid State Commun.* **51**, 263 (1984).
- ⁵C. S. Mononi, J. Z. Hu, and I. L. Spain (unpublished).
- ⁶M. T. Yin and M. L. Cohen, *Phys. Rev. B* **26**, 5668 (1982).
- ⁷K. J. Chang and M. L. Cohen, *Phys. Rev. B* **30**, 5376 (1984); **31**, 7819 (1985).
- ⁸R. Needs and R. Martin, *Phys. Rev. B* **30**, 5390 (1984).
- ⁹A. K. MaMahan and J. A. Moriarty, *Phys. Rev. B* **27**, 3235 (1983).
- ¹⁰K. J. Chang, M. Dacorogna, M. L. Cohen, J. M. Mignot, G. Chouteau, and G. Martinez, *Phys. Rev. Lett.* **54**, 2375 (1985).
- ¹¹M. Dacorogna, K. J. Chang, and M. L. Cohen, *Phys. Rev. B* **32**, 1853 (1985).
- ¹²D. Erskine, P. Y. Yu, K. J. Chang, and M. L. Cohen *Phys. Rev. Lett.* **57**, 2741 (1986).
- ¹³T. H. Lin, W. Dong, K. Dunn, C. Wagner, and F. Bundy, *Bull. Amer. Phys. Soc.* **31**, 640 (1986).
- ¹⁴Y. K. Vohra, K. E. Brister, S. Desgreniers, A. L. Ruoff, K. J. Chang, and M. L. Cohen, *Phys. Rev. Lett.* **56**, 1944 (1986).
- ¹⁵S. M. Sharma and S. K. Sikka, *J. Phys. Chem. Solids* **46**, 477 (1985).
- ¹⁶C. Kittel, *Introduction to Solid State Physics*, 5th ed. (Wiley, New York, 1976), p. 96.
- ¹⁷See references in Y. K. Vohra, K. E. Brister, S. Desgreniers, A. L. Ruoff, K. J. Chang, and M. L. Cohen, *Phys. Rev. Lett.* **56**, 1944 (1986).
- ¹⁸R. H. Wentorf and J. S. Kasper, *Science* **139**, 338 (1963).
- ¹⁹J. S. Kasper and S. M. Richards, *Acta Crystallogr.* **17**, 752 (1964).
- ²⁰F. P. Bundy and J. S. Kasper, *Science* **139**, 340 (1963).
- ²¹D. J. Chadi, *Phys. Rev. B* **32**, 6485 (1985).
- ²²A. Gruttner, R. Nesper, and H. G. von Schnering, *Angew. Chem.* **94**, 933 (1982) [*Angew. Chem. Int. Ed. Eng.* **21**, 912 (1982)].
- ²³M. L. Cohen, *Phys. Scr. T* **1**, 5 (1982).
- ²⁴E. Wigner, *Trans. Faraday Soc.* **34**, 678 (1938).
- ²⁵D. R. Hamann, M. Schlüter and C. Chiang, *Phys. Rev. Lett.* **43**, 1494 (1979).
- ²⁶M. T. Yin and M. L. Cohen, *Phys. Rev. B* **26**, 3259 (1982).
- ²⁷*Theory of Inhomogeneous Electron Gas*, edited by S.

- Lundqvist and N. H. March (Plenum, New York, 1983), and references therein.
- ²⁸G. B. Bachelet and N. E. Christensen, *Phys. Rev. B* **31**, 879 (1985).
- ²⁹K. M. Rabe and J. D. Joannopoulos, *Phys. Rev. B* **32**, 2303 (1985).
- ³⁰J. Ihm, A. Zunger, and M. L. Cohen, *J. Phys. C* **12**, 4401 (1979).
- ³¹M. Y. Chou, M. L. Cohen, and S. G. Louie, *Phys. Rev. B* **32**, 7979 (1985).
- ³²F. D. Murnaghan, *Proc. Nat. Acad. Sci.* **30**, 244 (1944).
- ³³M. T. Yin, in *Proceedings of the 17th International Conference on the Physics of Semiconductors, San Francisco*, edited by J. D. Chadi and W. A. Harrison (Springer-Verlag, New York, 1985), p. 927.
- ³⁴W. Paul, *J. Appl. Phys.* **32**, 2082 (1961).
- ³⁵K. J. Chang, S. Froyen, and M. L. Cohen, *Solid State Commun.* **50**, 105 (1984), and references therein.
- ³⁶*Semiconductors*, Vol. 17a of *Landolt Börnstein*, edited by O. Madelung, M. Schulz, and H. Weiss, (Springer-Verlag, Berlin, 1982), and references therein.
- ³⁷Y. K. Vohra and A. L. Ruoff (private communication).
- ³⁸M. J. Baublitz and A. L. Ruoff, *J. Appl. Phys.* **53**, 5669 (1982).
- ³⁹A. Jayaraman and R. C. Sherwood, *Phys. Rev.* **134**, A691 (1964).
- ⁴⁰M. L. Cohen, K. J. Chang, and M. M. Dacorogna, *Physica B* **135**, 229 (1985).
- ⁴¹K. K. Mon, N. W. Ashcroft, and G. V. Chester, *Phys. Rev. B* **19**, 5103 (1979).
- ⁴²J. R. Parsons and C. W. Hoelke, *Nature* **301**, 591 (1983); *Philos. Mag. A* **50**, 329 (1984).
- ⁴³C. Kittel, *Introduction to Solid State Physics*, Ref. 16, p. 442.
- ⁴⁴M. T. Yin and M. L. Cohen, *Phys. Rev. B* **29**, 6996 (1984).